Catalytic Mechanism of the *Streptomyces* K15 DD-Transpeptidase/Penicillin-Binding Protein Probed by Site-Directed Mutagenesis and Structural Analysis[†,‡]

Noureddine Rhazi,[§] Paulette Charlier,[||] Dominique Dehareng,[§] Danièle Engher,[§] Marcel Vermeire,[||] Jean-Marie Frère,[§] Martine Nguyen-Distèche,*[,§] and Eveline Fonzé*[,||]

Institut de Physique B5 and Institut de Chimie B6, Centre d'Ingénierie des Protéines, Université de Liège, B-4000 Sart Tilman, Belgium

Received November 27, 2002; Revised Manuscript Received January 15, 2003

ABSTRACT: The *Streptomyces* K15 penicillin-binding DD-transpeptidase is presumed to be involved in peptide cross-linking during bacterial cell wall peptidoglycan assembly. To gain insight into the catalytic mechanism, the roles of residues Lys38, Ser96, and Cys98, belonging to the structural elements defining the active site cleft, have been investigated by site-directed mutagenesis, biochemical studies, and X-ray diffraction analysis. The Lys38His and Ser96Ala mutations almost completely abolished the penicillin binding and severely impaired the transpeptidase activities while the geometry of the active site was essentially the same as in the wild-type enzyme. It is proposed that Lys38 acts as the catalytic base that abstracts a proton from the active serine Ser35 during nucleophilic attack and that Ser96 is a key intermediate in the proton transfer from the Oγ of Ser35 to the substrate leaving group nitrogen. The role of these two residues should be conserved among penicillin-binding proteins containing the Ser-Xaa-Asn/Cys sequence in motif 2. Conversion of Cys98 into Asn decreased the transpeptidase activity and increased hydrolysis of the thiolester substrate and the acylation rate with most β-lactam antibiotics. Cys98 is proposed to play the same role as Asn in motif 2 of other penicilloyl serine transferases in properly positioning the substrate for the catalytic process.

Bacterial wall peptidoglycan is a mesh-like structure in which short peptides cross-link linear strands of glycan consisting of alternating *N*-acetylglucosamine (GlcNAc) and *N*-acetylmuramic acid (MurNAc) residues. The carboxylic group of the MurNAc residue is amide-linked to the peptide unit L-Ala-γ-D-Glu-L-R_3-D-Ala. In *Streptomyces* K15, the L-R_3 residue is LL-diaminopimelic acid (LL-A_2pm) and the interpeptide bridge which extends from the C-terminal D-Ala of one peptide to the ϵ-amino group of the LL-A_2pm of another peptide is a glycine residue.

From the lipid II precursor, GlcNAcMurNAc (L-Ala-γ-D-Glu-L-R_3-D-Ala-D-Ala) P-P-undecaprenol, assembly of peptidoglycan requires two types of enzymatic activities: glycosyltransferases that catalyze glycan chain elongation and acyl serine transferases (transpeptidases) that catalyze peptide cross-linking (*1*). The transpeptidase reaction proceeds with the formation of a serine ester-linked peptidyl (L-Ala-γ-D-Glu-L-R_3-D-Ala) enzyme with concomitant release of the C-terminal D-Ala of the pentapeptide acting as a donor. The peptidyl moiety is then transferred to the side chain amino group of the L-R_3 residue of another peptide acting as an acceptor. The acyl serine transferases are the targets of penicillin action. They catalyze the opening of the β-lactam amide bond of penicillin with formation of penicilloyl serine enzymes that are easily detected. In consequence they are known as penicillin-binding proteins (PBPs).[1]

The bifunctional class A PBPs catalyze the polymerization of peptidoglycan in conjunction with other proteins (*2*, *3*). The multimodular class B PBPs are cell morphogenetic proteins, devoid of glycosyl transferase activity and involved with other components in peptidoglycan synthesis during cell division and elongation (*4*−*6*). During cell growth and division, the peptidoglycan is continuously remodeled by hydrolases. Monofunctional PBPs hydrolyze D-Ala-D-Ala bonds or interpeptide bridges. These DD-carboxypeptidases/PBPs control the extent of peptide cross-linking, allow the insertion of new material, and are involved in the cell shape maintenance and peptidoglycan recycling (*7*, *8*).

Bacteria have developed various strategies to protect their peptidoglycan assembly machineries against the toxic effect of β-lactams. One of the most prevalent mechanisms of resistance to penicillin is β-lactamase production (*9*). β-Lactamases of classes A, C, and D hydrolyze penicillin with

[†] This research was supported in part by the Belgian Program on Interuniversity Poles of Attraction initiated by the Belgian State, Prime Minister's Office, Science Policy Programming (PAI P5/33), and by the Fonds de la Recherche Fondamentale Collective Contracts 2.4537.99 and 2.4508.01. This work describes in part results obtained by N. Rhazi within the framework of his Ph.D. thesis (2000).

[‡] Atomic coordinates have been deposited in the Protein Data Bank (codes 1j9m, 1es2, 1es3, and 1es4) at Rutgers University.

* To whom correspondence should be addressed. E.F.: phone, 32.43.66.36.20; fax, 32.43.66.33.64; e-mail, eveline.fonze@ulg.ac.be.

[§] Institut de Chimie B6, Université de Liège.

[||] Institut de Physique B5, Université de Liège.

[1] Abbreviations: PBPs, penicillin-binding proteins; PDB, Protein Data Bank; rms, root mean square; Ac_2KAA, Ac_2-L-Lys-D-Ala-D-Ala; N^{α}-AcKAA, N^{α}-Ac-L-Lys-D-Ala-D-Ala; Ac_2KATl, Ac_2-L-Lys-D-Ala-thiolactate; N^{α}-AcKATl, N^{α}-Ac-L-Lys-D-Ala-thiolactate; PhacATl, phenylacetyl-D-Ala-thiolactate; PhacATg, phenylacetyl-D-Ala-thioglycolate; S2a, benzoyl-Gly-thioglycolate; S2c, benzoyl-Gly-thiolactate; S2d, benzoyl-D-Ala-thioglycolate.

10.1021/bi027256x CCC: $25.00
Published on Web 02/19/2003

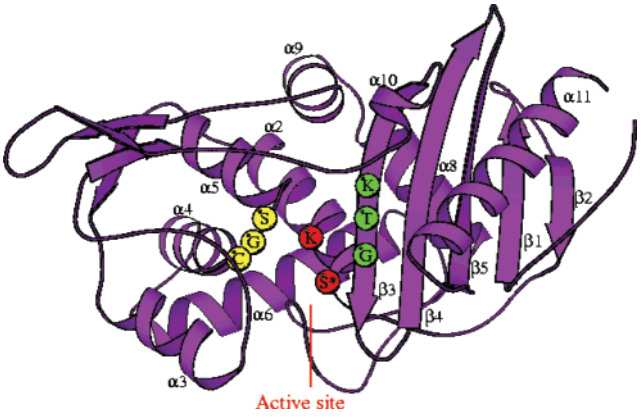

FIGURE 1: Ribbon diagram of the *Streptomyces* K15 penicillin-sensitive DD-transpeptidase and identification of the conserved residues of the active site including the nucleophilic serine S* residue.

the transient formation of penicilloyl serine enzymes. β-Lactamases and PBPs are members of the same penicilloyl serine transferase superfamily (*10*).

The monofunctional *Streptomyces* K15 DD-transpeptidase is a 262 amino acid PBP presumed to be involved in peptidoglycan cross-linking. Although lacking a membrane anchor, the protein is associated to the cytoplasmic membrane and in vitro requires 0.5 M NaCl to remain soluble (*11*). The rate of transpeptidation catalyzed by the K15 enzyme depends on the nature of both the scissile bond (peptide, thiolester, or ester) of the carbonyl donor and the acceptor. When assayed on Ac_2-L-Lys-D-Ala-D-Ala, the enzyme behaves as a poor hydrolase. It utilizes the small amount of released D-Ala as an acceptor to catalyze a silent exchange between the tripeptide C-terminal D-Ala and the free amino acid (*12*). In the presence of Gly-Gly or Gly-L-Ala, which mimic the structure of the acceptor in the nascent peptidoglycan, virtually no hydrolysis product is formed, and the enzyme behaves as a strict and efficient transpeptidase. By contrast, Ac_2-L-Lys-D-Ala-D-lactate is rapidly and completely hydrolyzed, D-lactate being a much poorer acceptor than D-Ala. But in the presence of Gly-Gly, the rate of utilization of the ester donor is also increased (*12*, *13*).

The structure of the K15 DD-transpeptidase has been elucidated at 2 Å resolution (*14*). The polypeptide is organized in two domains and adopts the same general fold as the other members of the penicilloyl serine transferase family of known 3D structures. One domain mainly contains α-helices; the second is of the α/β type. The catalytic pocket is located at the interface between the two domains and is mainly defined by three conserved motifs. Motif Ser35-Thr-Thr-Lys (motif 1 with the essential serine residue) of the α2 helix is central to the cavity. Motif Ser96-Gly-Cys (motif 2) on a loop connecting α-helices 4 and 5 is on one side of the cavity. Among the known penicilloyl serine transferases, the K15 enzyme is the only one with a cysteine as the third residue of motif 2. A few class A β-lactamases or multimodular class B PBPs have a glycine, serine, or aspartic acid in this position, and class D β-lactamases have a strictly conserved valine instead of the usual asparagine residue. Motif Lys213-Thr-Gly (motif 3) at the carboxy-terminal region of strand β3 is on the other side of the cavity (Figure 1).

Relative distances between the side chains of the active site defining motifs of the penicilloyl serine transferases are well conserved. However, there are a number of differences around the active site. Class A β-lactamases possess a fourth Glu166-Xaa-Xaa-Leu motif located at the bottom of the cavity (the Ω loop). Glu166 would play the role of general base in the hydrolysis of penicillins (*15*, *16*). PBPs and β-lactamases of classes C and D have no residue equivalent to glutamate 166. The *Streptomyces* R61 DD-carboxypeptidase/PBP (*17*) and the class C β-lactamases have a tyrosine in the first position of motif 2 which replaces the serine of all known PBPs, and β-lactamases of classes A and D have a serine at this position. The hydroxyl group of the tyrosine in the R61 enzyme and class C β-lactamases superimposes on that of the serine of class A β-lactamases and of the K15 enzyme, and its anion is proposed to act as the general base, compensating the absence of the class A Glu166 (*18*, *19*). Analysis of the 3D structure of class D β-lactamases and PBPs containing a serine in motif 2 revealed that there is no counterpart to the residues proposed to act as general bases in β-lactamases of classes A and C and the R61 enzyme. In the class D β-lactamases Lys70 of motif 1 is carbonated, and the carbamyl carboxylate is proposed to act as the general base in the catalytic mechanism (*20*−*22*). The identity of the general base in PBPs containing a serine residue in motif 2 (or of the Ser-Xaa-Asn type) is not yet clearly known. In this paper, the roles of Lys38 of motif 1 and Ser96 and Cys98 of motif 2 in the K15 DD-transpeptidase have been investigated by site-directed mutagenesis (Figure 1). The effects of the modifications were probed by analyzing the catalytic properties of the mutant enzymes, and their X-ray structures were compared to that of the wild-type enzyme.

MATERIALS AND METHODS

Materials. Ac_2-L-Lys-D-Ala-D-Ala was a gift from Reanol (Budapest, Hungary), and N^{α}-Ac-L-Lys-D-Ala-D-Ala, Ac_2-L-Lys-D-Ala-thiolactate, and N^{α}-Ac-L-Lys-D-Ala-thiolactate were gifts from UCB-Bioproducts (Braine-l'Alleud, Belgium). Thiolesters benzoyl-Gly-thioglycolate, benzoyl-Gly-thiolactate, and benzoyl-D-Ala-thioglycolate were synthesized as described (*23*, *24*). Phenylacetyl-D-Ala-thiolactate and phenylacetyl-D-Ala-thioglycolate were gifts from Aventis (Romainville, France). Benzylpenicillin, piperacillin, oxacillin, cephalothin, and cefoxitin were from Sigma, and carbenicillin and cephalosporin C were gifts from Beecham and Glaxo, respectively. Chemical structures are shown in Schemes 1 and 2.

Recombinant Plasmids. (1) pDML2104. The 1357 bp *Sph*I fragment carrying the K15 DD-peptidase encoding gene was excised from plasmid pDML225 (*11*) and inserted into the corresponding sites of pUC19. The resulting plasmid called pDML2100 was used as template to introduce a *Nco*I site at the 5′ end of the K15 enzyme (Val1 to Leu262) encoding gene by site-directed mutagenesis (QuickChange Mutagenesis Kit, Stratagene) using the oligonucleotide 5′actcccgcgaccatggaccaagcccaccatcg3′ and its reverse. The modified gene was sequenced to detect potential errors. The 1066 bp *Nco*I−*Sac*I fragment was excised from pDML2100/*Nco*I and inserted into the corresponding sites of plasmid pET28a(+) (Novagen), giving rise to pDML2104. The gene encoding the K15 DD-transpeptidase, which contained one additional

Scheme 1: Structures of the Substrates

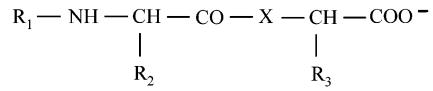

Substrate	R_1[a]	R_2	R_3	X
Ac_2KAA	Ac_2K	$CH_3(D)$	$CH_3(D)$	NH
αAcKAA	AcK	$CH_3(D)$	$CH_3(D)$	NH
Ac_2KATl	Ac_2K	$CH_3(D)$	$CH_3(D)$	S
αAcKATl	AcK	$CH_3(D)$	CH_3	S
PhacATl	C_6H_5-CH_2-CO	$CH_3(D)$	CH_3	S
PhacATg	C_6H_5-CH_2-CO	$CH_3(D)$	H	S
S2a	C_6H_5-CO	H	H	S
S2c	C_6H_5-CO	H	$CH_3(D)$	S
S2d	C_6H_5-CO	$CH_3(D)$	H	S

[a] Ac and K are acetyl and L-lysyl, respectively.

N-terminal methionine, was under the control of the T7 promotor, lac operator.

(2) pDML2108 and pDML2107. Plasmid pDML2100 was used as template for site-directed mutagenesis (QuickChange Mutagenesis, Stratagene) using oligonucleotides 5′ctgatgctgccggccggctgcgacg3′ and 5′ggcgtcgcagccggccggcagcatcagc3′ (Ser96Ala mutation) and 5′ctgccgtccggcaacgacgccgcgtacgcg3′ and 5′gtacgcggcgtcgttgccggacggcagc3′ (Cys98Asn mutation). After sequencing of the modified region, the *Sac*I−*Sac*II 984 bp segment was exchanged with the corresponding unmodified fragment of pDML2104, giving rise to pDML2108 encoding the S96A K15 DD-peptidase. The 1357 bp *Sph*I fragment (carrying the Cys98Asn mutation) was inserted into the same site of pIJ702 (*25*). The resulting plasmid pDML2107 encoded the Cys98Asn enzyme.

(3) pDML2105 and pDML2106. The overlap extension PCR method was used to introduce the Lys38His and Cys98Ala mutations (*26*). In separate PCRs, two fragments of the target gene were amplified. The first reaction used the flanking primer 5′cgcctccgtagagctgccg3′ which hybridized downstream from the K15 encoding gene and the internal antisense primer 5′cggtcatgatgtgggtggtggagcc3′ (Lys38His mutation) or 5′ggcgtcggcgccggacggc3′ (Cys98Ala mutation) which hybridized with the site of mutation. The second reaction used the flanking antisense primer 5′gcgaagacgaggcagtacttgc3′ which hybridized upstream of the K15 DD-transpeptidase encoding gene and the internal sense primer 5′ccaccacccacatcatgaccgcca3′ (Lys38His mutation) or 5′gtccggcgccgacgccgc3′ (Cys98Ala mutation) which hybridized with the site of mutation. The reaction mixture contained 50 μg of pDML2100, the DNA template, 100 pmol of each primer, 200 μM dNTPs, 0.5 unit of Vent DNA polymerase, and 10 μL of DMSO in 100 μL of the recommended buffer. Thirty cycles of PCR were performed as follows: 1 min at 95 °C, 30 s at 58 °C, and 1 min at 72 °C. The two fragments were purified by agarose gel electrophoresis and fused by denaturating and annealing them in a subsequent primer extension reaction. By addition of extra flanking primers, the 764 bp fragment was further amplified by PCR (see above), purified, digested with the restriction enzymes *Eag*I and *Bpu*1102I, and exchanged with the corresponding fragment of pDML2100. The 1357 *Sph*I DNA fragment was completely sequenced and inserted into the *Sph*I site of pIJ702 (*25*). The resulting plasmids pDML2105 and pDML2106 encoded the Lys38His and Cys98Ala mutants, respectively.

Production and Purification of the K15 DD-Transpeptidase and Derivatives. Mutants Lys38His, Cys98Ala, and Cys98Asn were produced by *Streptomyces lividans* TK24 (*27*) harboring the appropriate plasmid and purified as described previously (*11*). The final yield was about 2−4 mg of 95% pure enzyme/L of culture and was similar to that of the wild-type protein produced by *S. lividans* (*11*, *13*).

The wild-type enzyme and the Ser96Ala mutant were produced in the cytoplasm of *Escherichia coli* BL21(DE3) (Novagen, Oxon, U.K.) harboring pDML2104 or pDML2108. The cells were grown at 37 °C in Luria−Bertani medium containing 50 μg/mL kanamycin. When the A_{600} reached a value of 0.8, the culture was supplemented with 1 mM IPTG and maintained at 18 °C during 16 h. The *E. coli* cells were suspended in 25 mM Tris-HCl, pH 7.2, containing 0.2 mM DTT and 0.4 M NaCl, and disrupted at 4 °C in a cell desintegrator (Constant System, Warwick, U.K.). After centrifugation at 30000*g* for 30 min, the supernatant was incubated at 4 °C in the presence of benzonase and 2 mM $MgCl_2$. The preparation was then dialyzed against Tris-HCl/DTT buffer without NaCl, and the purification was performed as described previously (*11*). The final yield was 30 mg of 95% pure enzyme (wild type or Ser96Ala mutant)/L of culture, about 10 times higher than that obtained with *S. lividans* TK24 harboring pDML225. The wild-type enzyme produced in *E. coli* showed the same properties (thermostability, affinity for β-lactams, activity toward the peptide and thiolester substrates) as the enzyme produced in *S. lividans* TK24.

Enzymatic Activity Measurements. The peptides and the enzyme were incubated at 37 °C in 5.7 mM Tris-HCl, pH 7.2, containing 0.045 mM DTT and 0.1 M NaCl. The released D-Ala was measured by the D-amino acid oxidase procedure (*28*).

The thiolesters and the enzyme were incubated at 37 °C in 25 mM sodium phosphate, pH 7.2, containing 4 μM DTT and 0.4 M NaCl. The steady-state parameters k_{cat}, K_m, and k_{cat}/K_m were estimated as described (*13*).

The carbonyl donor benzoyl-D-Ala-thioglycolate (D), the hydrolyzed product (H), and the aminolysed product (T) of the transfer reaction in the presence of D-Ala were separated by HPLC on a ET250/8/4 Nucleosil 5C18 column (Macherey-Nagel). The flow rate was 1 mL/min. The retention times for D, H, and T were 54, 27, and 34 min, respectively (under isocratic conditions using 5% acetonitrile in 10 mM sodium acetate, pH 3.0. Detection was performed at 235 nm. The transfer to hydrolysis ratio was quantified as described (*24*, *28*).

Inactivation of the K15 enzyme (E) by β-lactam compounds (I) was interpreted on the basis of the reaction model:

$$E + C \underset{k_{-1}}{\overset{k_{+1}}{\rightleftarrows}} EI \xrightarrow{k_2} EI^* \xrightarrow{k_3} E$$

where EI is the Henri−Michaelis complex, EI* the covalent acyl-enzyme, and P the degradation product of the β-lactam. The k_2 and k_3 parameters are first-order rate constants, and

Scheme 2: Structures of the Antibiotics

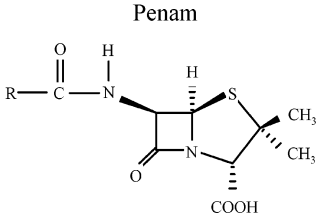

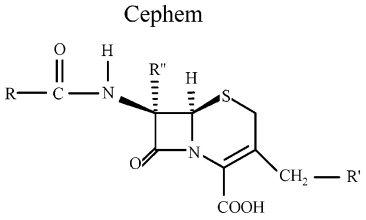

Substrates	R	R'	R"
Benzylpenicillin	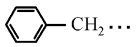		
Carbenicillin	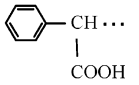		
Oxacillin	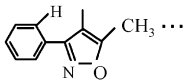		
Piperacillin	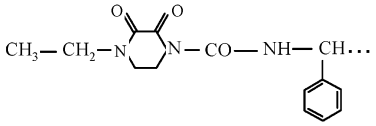		
Cephalosporin C	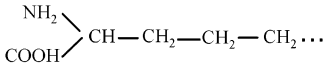	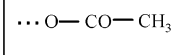	
Cephalothin	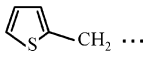	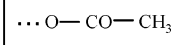	
Cefoxitin	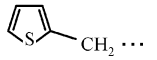	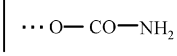	

k_2/K is the second-order rate constant for enzyme acylation (*30*). The k_2 parameter is negligible when compared to k_{-1} so that $K' = [(k_{-1} + k_2)/k_{+1}] = [k_{-1}/k_{+1}] = K$, the dissociation constant of EI.

The k_2/K parameter was determined as described (*29*) or with benzoyl-D-Ala-thiolglycolate or phenylacetyl-D-Ala-D-thiolactate as reporter substrates (*28*). The rate of deacylation (k_3) was determined as described (*30*). The labeling of the K15 enzyme with [^{3}H]benzylpenicillin (18 Ci/mmol, Radiochemical Centre, Amersham, U.K.) was estimated as described (*31*).

Thermal Denaturations. The enzyme (10 μM) was incubated at 60 °C in 25 mM Tris-HCl, 0.2 mM DTT, and 0.4 M NaCl during various periods of time. The residual activity was measured at 37 °C using the cosubstrates Ac$_2$-L-Lys-D-Ala-D-Ala (5 mM) and Gly-Gly (10 mM). Alternatively, the time-dependent decrease in protein fluorescence at 72 °C was monitored using a Perkin-Elmer LS50 spectrophotometer (excitation, 280 nm; emission, 330 nm). The enzyme concentration was 1 μM.

X-ray Crystallography. The crystals of the modified K15 enzyme were obtained at 20 °C by the hanging drop vapor diffusion method under conditions similar to those described for the wild-type enzyme (*14*). The modified proteins (2.3−20 mg/mL) crystallized in the presence of various concentrations of poly(ethylene glycol) 6000 (PEG) as precipitating agent, in 0.1 M Tris-HCl, pH 7.2, and 0.5 M NaCl, except for the Cys98Ala mutant which crystallized in a PEG solution buffered with 0.1 M 2-(*N*-morpholino)ethanesulfonic acid (MES)−HCl, pH 6.0. The crystals of the Lys38His, Ser96Ala, and Cys98Ala/Asn mutants grew as small prisms and, like the original native enzyme crystals, belonged to the orthorhombic space group $P2_12_12_1$ with similar unit cell dimensions (Table 1).

X-ray diffraction experiments were carried out at room temperature (Cys98Ala and Cys98Asn mutants) or under cryogenic conditions (100 K) after the crystals were transferred to adequate cryosolvents (Lys38His and Ser96Ala mutants). Data for the Lys38His, Ser96Ala, and Cys98Ala mutants were collected on a Siemens X1000 area detector with a Rigaku RU-200 rotating anode generator operating at 50 kV and 90 mA (λ = 1.5418 Å). They were then indexed, integrated, scaled, and merged using the SAINT software (*32*). Data for the Cys98Asn mutant and to higher resolution for the Ser96Ala mutant were obtained at LURE (Laboratoire pour l'Utilisation du Rayonnement Synchrotron, Orsay, France) on beamline D41-A (λ = 1.375 Å) using a MARResearch Mar300 imaging plate. These data were indexed and integrated with MOSFLM (*33*). The scaling and reducing steps were accomplished using the SCALA and TRUNCATE programs (*34*). To improve the data quality for the Lys38His mutant, new data were collected at ESRF (European Synchrotron Radiation Facility, Grenoble, France) on beamline ID14-3 (λ = 0.933 Å) using a MAR 165 mm CCD detector, and they were entirely processed using the

Table 1: Diffraction Data Collection and Processing[a]

	mutant			
	Lys38His	Ser96Ala	Cys98Ala	Cys98Asn
space group $P2_12_12_1$				
a (Å)	45.57	45.28	46.30	46.04
b (Å)	53.64	53.15	54.09	53.74
c (Å)	104.69	104.70	108.77	107.96
resolution range (Å)				
overall reflections	34.71−1.56	41.56−1.50	42.60−2.13	22.69−1.88
highest resolution shell	1.60−1.56	1.55−1.50	2.20−2.13	1.93−1.88
no. of unique reflections	34332 (1069)	38470 (2624)	14472 (730)	20385 (1634)
completness (%)	91.7 (39.7)	87.9 (85.0)	90.6 (46.8)	89.8 (95.6)
redundancy	3.7	4.1	3.5	3.7
$\langle I/\sigma(I)\rangle$	19.3 (4.1)	12.1 (6.1)	4.2 (ND)[b]	8.7 (4.1)
R_{merge}[c] (%)	3.8 (13.9)	4.6 (10.5)	4.4 (18.3)	6.1 (18.2)

[a] Data for the highest resolution shell are in parentheses. [b] ND stands for not determined. [c] $R_{merge} = \sum_{hkl}|I_{hkl} - \langle I_{hkl}\rangle|/\sum_{hkl}I_{hkl}$, where I_{hkl} is the measured intensity of the reflection with the indices *hkl*.

Table 2: Refinement Statistics

	mutant			
	Lys38His	Ser96Ala	Cys98Ala	Cys98Asn
resolution range (Å)	8.00−1.65	8.00−1.55	10.00−2.20	8.00−1.90
completeness (%)	96.9	92.7	89.3	84.1
no. of unique reflections[a]	30376	34434	12742	18050
R^b (working set) (%)	21.8	22.5	17.4	17.9
R_{free} (test set) (%)	25.6	27.0	24.5	22.5
protein atoms (non-H)	1928	1912	1912	1900
heterogen and solvent atoms	199	252	131	144
B values from Wilson plot (Å^2)	17.1	14.2	23.5	13.6
mean *B* value (overall, Å^2)	15.0	11.9	20.7	17.0
estimated coordinate error (low-resolution cutoff of 5.0 Å) from Luzzati plot/sigmaA (Å)	0.21/0.17	0.20/0.16	0.22/0.23	0.18/0.16
rms deviations from ideal values				
bond lengths/angles (Å/deg)	0.007/1.2	0.006/1.2	0.007/1.2	0.006/1.2
dihedral/improper angles (deg/deg)	24.6/0.66	24.3/0.67	26.2/0.60	25.7/0.63

[a] Reflections $F < 2\sigma$ are rejected in the Lys38His and Ser96Ala mutants, and for the Cys98Ala and Cys98Asn mutants, a cutoff of 3 was applied. [b] $R = \sum_{hlk}||F_{o,hkl}| - |F_{c,hkl}||/\sum_{hlk}F_{o,hkl}$, where $|F_{o,hkl}|$ and $|F_{c,hkl}|$ are the observed and calculated structure factor amplitudes.

XDS package (*35*). Data collection statistics are shown in Table 1.

Since all crystals of the K15 derivatives were isomorphous with those of the wild-type enzyme (PDB entry 1SKF), their crystallographic structures were solved by the classical difference Fourier method using the native K15 enzyme coordinates. The verification of the mutated residues was carried out using the combination of omit maps and difference maps. The standard refinement procedure employing X-PLOR (*36*) and model building in the electron density maps with TURBO-FRODO (*37*) were applied to each mutant, yielding the final refined structures (Table 2). Coordinates have been deposited in the Brookhaven Protein Data Bank with accession codes 1J9M, 1ES2, 1ES3, and 1ES4 for the Lys38His, Ser96Ala, Cys98Ala, and Cys98Asn K15 enzymes, respectively.

RESULTS

Production, Stability, and Physical Properties of the Modified K15 DD-*Transpeptidase.* The Ser96Ala K15 enzyme was produced in the cytoplasm of *E. coli* BL21(DE3) harboring pDML2108 whereas all of the other K15 enzyme derivatives were produced in the culture medium *of S. lividans* harboring the appropriate vector. The modified proteins were purified to 95%, and the behavior of the proteins was similar to that of the native one in all purification steps. One may note that the production in *E. coli* was 10 times higher than in *S. lividans* (30 mg/L of culture versus 3 mg/L). The modified proteins were indistinguishable from the native enzyme with respect to their absorption (210−340 nm), fluorescence (excitation at 280 nm), and circular dichroism (205−260 nm) spectra.

Incubation at 60 or 72 °C resulted into the time-dependent irreversible denaturation of the protein, which could be monitored by enzymatic activity or fluorescence measurements, respectively. The thermostability of the mutant enzymes reflects that observed for the wild-type protein at both temperatures. The half-lives were 3.5 ± 0.5 (Lys38His), 8 ± 2 (Ser96Ala), 6 ± 1 (Cys98Asn), 13 ± 2 (Cys98Ala), and 10 ± 2 (wild type) min at 72 °C by fluorescence measurements and 120 ± 20 (Ser96Ala), 220 ± 10 (Cys98Ala), 30 ± 4 (Cys98Asn), and 170 ± 40 (wild type) min at 60 °C by enzymatic activity measurements.

Interaction of the K15 DD-*Transpeptidase Mutants with β-Lactams.* Table 3 compares the antibiotic sensitivity profiles of the wild-type and the modified K15 DD-transpeptidases. The Lys38His enzyme failed to bind β-lactams. No [^{3}H]benzylpenicillin binding activity was detected throughout the investigated pH range (from 3 to 11). The Ser96Ala enzyme was also inactive in terms of β-lactam binding with

Table 3: Interactions of Antibiotics with the K15 Wild-Type and Mutant Enzymes

	WT[a]		Ser96Ala		Cys98Ala		Cys98Asn	
antibiotic	k_2/K ($M^{-1}\cdot s^{-1}$)	$k_3 \times 10^{-5}$ (s^{-1})	k_2/K ($M^{-1}\cdot s^{-1}$)	$k_3 \times 10^{-5}$ (s^{-1})	k_2/K ($M^{-1}\cdot s^{-1}$)	$k_3 \times 10^{-5}$ (s^{-1})	k_2/K ($M^{-1}\cdot s^{-1}$)	$k_3 \times 10^{-5}$ (s^{-1})
benzylpenicillin	135	10	<0.1	ND[b]	115	8	130	28
carbenicillin	37	2.6	<0.1	ND	28	26	106	18
oxacillin	8	1.2	<0.05	ND	41	13	300	25
piperacillin	130	26	<0.1	ND	445	22	1100	68
cephalosporin C	0.7	2.3	<0.1	ND	1	4.2	7	9
cephalothin	2	<2.5	<0.05	ND	24	16	350	40
cefoxitin	720	1.7	0.23	0.014	400	27	7500	120

[a] See ref *30*. ND: not determinable; no acyl-enzyme was isolated.

Table 4: Interaction of Substrates with the K15 Wild-Type and Mutant Enzymes

		transpeptidation		hydrolysis						
enzyme		Ac_2KAA	αAcKAA	Ac_2KATl	αAcKATl	PhacATl	PhacATg	S2a	S2c	S2d
WT[c]	k_{cat} (s^{-1})	0.3	0.45	>0.43	0.1	0.6	>0.5	>0.024	0.017	0.11
	K_m (mM)	6.2	9.4	>3	0.4	1.2	>3	>3	0.22	1.5
	k_{cat}/K_m ($M^{-1}\cdot s^{-1}$)	50	48	145	250	460	160	8	75	75
Lys38His	k_{cat} (s^{-1})	≪0.3	≪0.3	≪0.1	≪0.1	>0.003	0.015	≪0.1	0.006	>0.015
	K_m (mM)	ND[a]	ND[a]	ND[b]	ND[b]	>3	2.4	ND[b]	1.0	>3
	k_{cat}/K_m ($M^{-1}\cdot s^{-1}$)	≪0.0004	≪0.001	≪0.1	≪0.1	1.1	6.4	≪0.1	6.0	5.0
Ser96Ala	k_{cat} (s^{-1})	>0.009	>0.005	>0.02	>0.02	>0.012	>0.024	>0.007	>0.045	>0.012
	K_m (mM)	>35	>35	>3	>3	>3	>3	>3	>3	>3
	k_{cat}/K_m ($M^{-1}\cdot s^{-1}$)	0.27	0.15	6.8	7.6	4.0	8.0	2.4	15.0	4.0
Cys98Ala	k_{cat} (s^{-1})	>0.2	0.13	1.1	0.8	2.2	>0.87	0.08	0.08	0.3
	K_m (mM)	>35	30	2.0	0.6	1.2	>3	0.8	0.3	1.3
	k_{cat}/K_m ($M^{-1}\cdot s^{-1}$)	6	4.3	580	1300	2000	290	100	270	200
Cys98Asn	k_{cat} (s^{-1})	>0.035	>0.02	>0.57	>0.9	>2.4	>0.96	>0.25	0.45	>0.8
	K_m (mM)	>35	>35	>3	>3	>3	>3	>3	3.3	>3
	k_{cat}/K_m ($M^{-1}\cdot s^{-1}$)	1.0	0.7	190	290	800	320	85	140	260

[a] Significantly less than 10% of the substrate was utilized when the enzyme (3 μM) was incubated in the presence of donor (35 mM) and acceptor (10 mM) substrates during 1 h. The maximum k_{cat} and k_{cat}/K_m values were computed on the assumption that the K_m value was much lower or much larger than 35 mM, respectively. [b] Significantly less than 10% of the substrate was utilized when the enzyme (3 μM) was incubated in the presence of thiolester substrates (3 mM) during 20 min. The maximum k_{cat} and k_{cat}/K_m values were computed on the assumption that the K_m value was much lower or much larger than 3 mM, respectively. [c] See ref *13*.

the exception of cefoxitin, for which a residual activity was detected. The value of the second-order acylation rate constant (k_2/K') was decreased by a factor of 3000 (0.23 $M^{-1}\cdot s^{-1}$ versus 720 $M^{-1}\cdot s^{-1}$ for the wild-type enzyme), and that of the deacylation rate constant (k_3) was decreased 120-fold (0.014×10^{-5} s^{-1} versus 1.7×10^{-5} s^{-1}). The k_2/K values of the Cys98Ala mutant were not very different from those of the wild-type enzyme with the exception of the cephalotin, oxacillin, and piperacillin values which were increased 5−10-fold. By contrast, the acylation rate constants of the Cys98Asn mutant by most of the β-lactams were increased 10−70-fold compared to the wild-type enzyme. The deacylation rate constant values of the Cys mutants also increased 2−70-fold.

Interaction of the K15 DD*-Transpeptidase Mutants with Substrates.* Table 4 compares the substrate profiles of the wild-type and the modified K15 DD-transpeptidases. The activities of the Lys38His and Ser96Ala mutants were very impaired. In some cases, the individual values of k_{cat} and K_m could not be determined because the K_m values were too high.

The Lys38His DD-transpeptidase catalyzed the aminolysis of Ac_2- (or αAc-) L-Lys-D-Ala-D-Ala in the presence of Gly-Gly or Gly-L-Ala with an extremely low efficiency. The k_{cat}/K_m values were decreased by 3−4 orders of magnitude. The Lys38His mutation also affected the efficiency of thiolester substrate hydrolysis. The k_{cat}/K_m values were decreased 15−400-fold. The extremely low activity of the Lys38His enzyme did not allow measurement of the pH dependence of the kinetic parameters. No aminolysis of the thiolester substrate benzoyl-D-Ala-thioglycolate (1 mM) by the Lys38His mutant was observed in the presence of D-Ala (0.1−10 mM).

The Ser96Ala mutant had a much decreased aminolysis activity. The catalytic efficiency represented 0.3−0.5% of that of the native enzyme with Ac_2- (or αAc-) L-Lys-D-Ala-D-Ala and Gly-Gly or Gly-L-Ala. The hydrolysis of thiolester substrates was less affected, 1−30% of that of the wild-type enzyme. The ratio between the aminolysis (T) and hydrolysis (H) products was determined as a function of the D-Ala concentration using benzoyl-D-Ala-thioglycolate as donor substrate (Table 5). This ratio increased proportionally to the concentration of D-Ala from 0.8 to 10 mM and was much lower for the Ser96Ala mutant than for the wild-type enzyme. Aminolysis, which represented 0.045% of that of the wild type, was more severely affected by the mutation than hydrolysis, which represented 0.4% of that of the wild type in the presence of 2 mM D-Ala.

The Cys98Asn and Cys98Ala DD-transpeptidases catalyzed the aminolysis of peptide donors in the presence of Gly-Gly or Gly-L-Ala with a decreased catalytic efficiency, 2−10% of that of the wild-type enzyme. In contrast, they catalyzed the hydrolysis of thiolester substrates with an increased catalytic efficiency, 130−1250% of that of the native enzyme. In the presence of benzoyl-Gly-thiolactate, the

Table 5: Ratios between the Aminolysis Product (T) and Hydrolysis Product (H)[a]

[D-Ala] (mM)	T/H ratio			
	WT[b]	Ser96Ala	Cys98Ala	Cys98Asn
0.8	4.1 ± 0.5	ND[c]	ND	0.56 ± 0.02
1	ND	0.5 ± 0.05	4.5 ± 0.3	0.86 ± 0.04
2	10.6 ± 1.5	1 ± 0.1	8.5 ± 0.4	1.20 ± 0.10
3	12.4 ± 1.8	ND	13.2 ± 0.4	2.03 ± 0.25
3.5	20.6 ± 5.1	ND	14.5 ± 0.6	2.60 ± 0.25
4	ND	1.23 ± 0.2	16.9 ± 0.8	2.94 ± 0.40

[a] Enzyme concentration was 1.38 μM (WT, Cys98Ala/Asn) or 4.6 μM (Ser96Ala), and incubation was 30 min (WT, Cys98Ala/Asn) or 3 h (Ser96Ala) in the presence of 1 mM benzoyl-D-Ala-thioglycolate and increasing concentrations of D-Ala. [b] See ref *13*. [c] ND: not determined.

Cys98Asn mutation increased both the k_{cat} value (0.45 versus 0.017 s^{-1}) and the K_m value (3.3 versus 0.22 mM), and the Cys98Ala mutation increased only the k_{cat} value (0.08 versus 0.017 s^{-1}). The Cys98Asn mutation had no major effect on the aminolysis of benzoyl-D-Ala-thiolglycolate in the presence of D-Ala whereas it increased the hydrolysis activity so that the T/H ratio decreased (14% of that of the native enzyme). In contrast, the Cys98Ala mutant hydrolyzed and aminolysed the benzoyl-D-Ala-thioglycolate with similar efficiencies which were 4 to 5 times higher than those of the wild-type enzyme. In consequence, the T/H ratio was not much modified (Table 5).

Overall Structure of the Modified K15 DD-*Transpeptidase.* The mutations had no major effect on the overall structure of the K15 enzyme. When the mutant structures were superimposed onto that of the native enzyme, the root-mean-square (rms) deviations for all equivalent atoms were distributed from 0.40 to 0.72 Å. For the equivalent backbone atoms (N, Cα, Cβ, C, O), the rms deviations ranged from 0.23 to 0.52 Å. Those values are relatively low, and only one significant change occurs in the Ser110-Phe121 loop connecting α5 to α6, which is directly involved in crystallographic packing interactions between symmetry-related molecules. In diffraction experiments, the Lys38His and Ser96Ala crystals were flash frozen at 100 K whereas the native enzyme X-ray data were collected at room temperature (unit cell parameters: $a = 46.59$ Å, $b = 54.53$ Å, and $c = 108.70$ Å). This thermal constraint induced a compression of the crystallographic cell in all three directions of about 2−3% along the *a* and *b* axes and 4% along the *c* axis (see Table 1). Consequently, the Ser110−Phe121 polypeptide chain was slightly shifted along the *a* axis in both Lys38His and Ser96Ala structures in comparison with the wild-type K15 and the Cys98Ala/Asn mutant structures. A similar modification was observed for the Lys61−Asn71 region.

No drastic modification of the active site geometry was observed, and the positions of the key residues were highly conserved (Figure 2a,c and Figure 3a,b). In the crystals of the wild-type and mutant enzymes, the electron density associated with the Ile145−Gly148 loop was always very poor, reflecting a relatively high disorder. Moreover, for the Lys38His and Cys98Asn mutants, three amino acid residues of the 145−148 loop were omitted during the refinement process (respectively Ile145-Gly146-Asn147 and Gly146-Asn147-Gly148). This disorder might be explained by the presence of two glycine residues, which are more flexible, and the lack of crystallographic packing constraints at that position. The hydrogen-bonding pattern in the catalytic cleft is also quite well conserved as shown in Table 6. In contrast to the other penicilloyl serine transferases, the orientation of the hydroxyl group of the active serine Ser35 is oriented away from Lys38 of motif 1, in a position incompatible with a favorable H-bonding interaction. Its position toward the β3 strand is stabilized by a H-bond with the main chain nitrogen atom of Ser216 (downstream of the motif 3 Lys-Thr-Gly triad) and a water molecule (Wat336) that could be compared to that found in the oxyanion hole of other penicilloyl serine transferases, although it is less buried. In the mutant structures the solvent content undergoes some modification, especially in the Ser96Ala mutant where a water molecule is occupying the position of the missing hydroxyl group of the serine side chain (Figure 2c). In the Cys98Asn mutant, the asparagine residue has a relative position more or less equivalent to that of Asn132 in the NMCA class A carbapenemase from *Enterobacter cloacae* where, in comparison with classical class A enzymes, a displacement of this residue in the active site by 1 Å enlarges the substrate binding pocket to accommodate carbapenem antibiotics (Figure 3c) (*38*).

Table 6: Catalytic Cleft Distances

amino acid/water identification		distance (Å)				
		WT	Lys38-His	Ser96-Ala	Cys98-Ala	Cys98-Asn
Ser35 OG	Ser216 N	3.0	3.0	3.1	3.0	3.0
	Wat336[a]	3.0	2.6	2.8	2.8	3.1
Lys38 NZ	Ser96 OG	3.0			3.4	3.6
	Cys98 SG	2.7		2.9		
	Asn98 OD1					2.6
	Wat524[b]			2.7		
His38 NE2	Ser96 OG		4.2			
	Cys98 SG		3.6			
Ser96 OG	Lys213 NZ	2.9	2.9		2.8	2.9
Wat524	Lys213 NZ			2.9		

[a] The corresponding water molecule in the Lys38His mutant is numbered 332. [b] Wat524 occupies the Ser96 hydroxyl group position in the Ser96Ala mutant.

DISCUSSION

The serine β-lactamases, the monofunctional PBPs, and the penicillin-binding modules of multimodular PBPs fulfill different functions and catalyze distinct reactions. However, they all operate on $R_1-CO-X-R_2$ carbonyl donors by a similar double proton shuttle. During the enzyme acylation, the proton of the active site serine γOH is transferred to the leaving group $X-R_2$ with concomitant nucleophilic attack of the carbonyl carbon of the donor by the activated Oγ. In the deacylation step, the proton of the acceptor (an amino group or a water molecule) is abstracted, the activated acceptor attacks the carbonyl carbon of the acyl-enzyme, and the abstracted proton is back-donated to the active site serine Oγ. The catalytic mechanism of the penicilloyl serine transferases has been investigated in great detail by site-directed mutagenesis and crystallographic, kinetic, and theoretical studies, allowing a definition of the role played by some amino acids found in the three conserved motifs [Ser-Xaa-Xaa-Lys, Ser/Tyr-Xaa-Asn/Val/Cys, and Lys/His-Thr/Ser-Gly] defining the catalytic pocket. As found in all serine proteases, the assisting catalytic mechanism

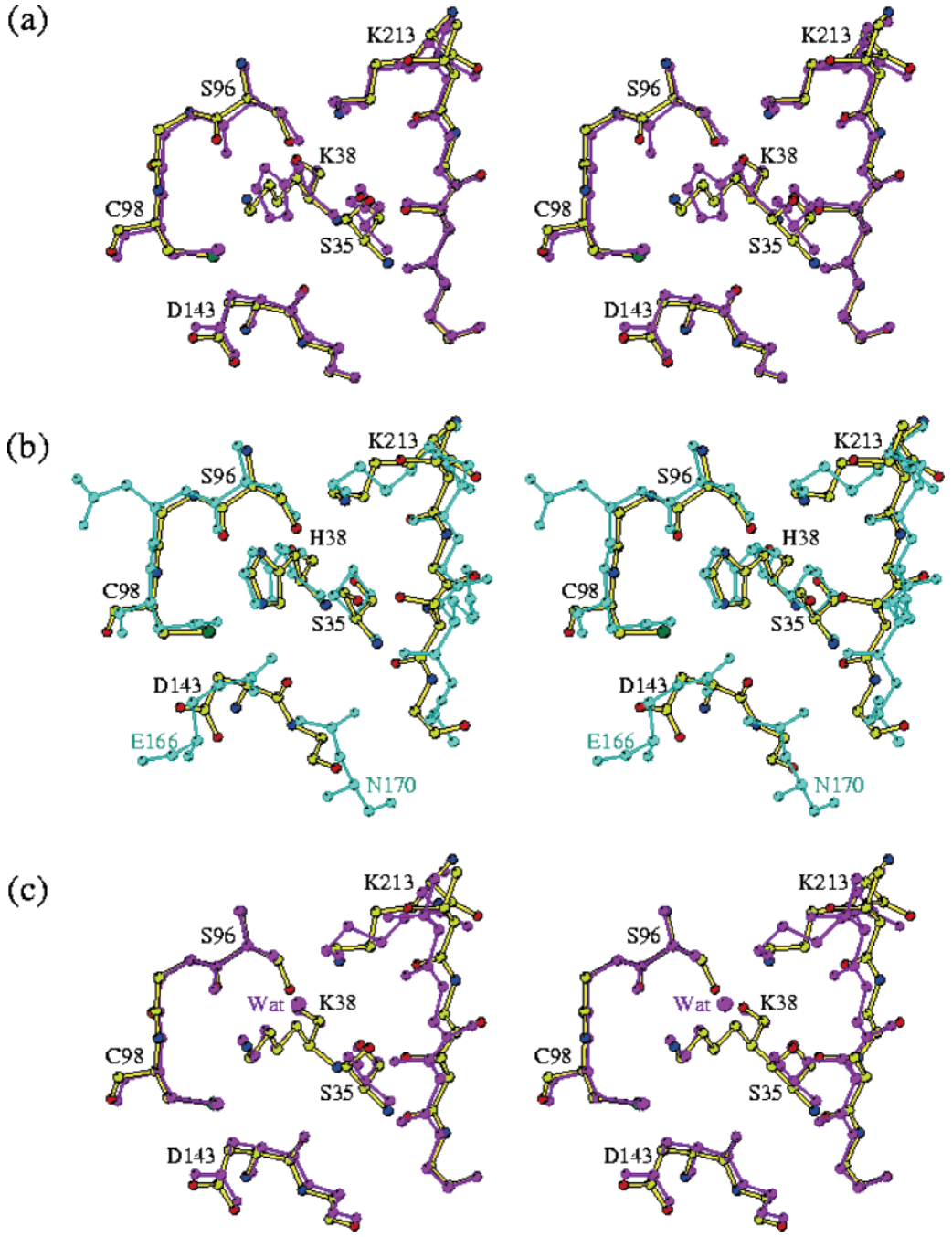

FIGURE 2: Superimposed active sites of (a) the K15 wild-type enzyme and its Lys38His mutant (magenta), (b) the K15 Lys38His mutant and the corresponding Lys73His mutant of the *S. aureus* class A β-lactamase (*56*) (cyan), and (c) the K15 wild-type enzyme and its Ser96Ala mutant (magenta).

includes an oxyanion hole defined by the backbone NH groups of the active serine and of the residue following motif 3.

In the class A β-lactamases, a fourth motif Glu166-Xaa-Glu-Leu-Asn defining the so-called Ω loop at the bottom of the catalytic cleft is a unique characteristic. There is now a consensus on the fact that the conserved Glu166 is the general base in the acylation and deacylation steps (*16*). The role played by Ser130 and Asn132 of motif 2 has also been intensively studied by site-directed mutagenesis (*39*−*42*). Catalytic data, computed interactions from modeling, and structural studies have confirmed that Ser130 has a structural role by maintaining a functional active site geometry as well as a critical role in substrate binding and specificity and that Asn132 is pivotal for the adequate positioning of the substrate for the nucleophilic attack by the active serine.

In the class C β-lactamases and the PBP of *Streptomyces* R61, where motif 2 is the Tyr-Xaa-Asn triad, it was proposed that the phenolate anion of tyrosine (respectively Tyr150 and Tyr159) acts as the general base responsible for the activation of the active serine during the acylation step and for the subsequent activation of the catalytic water molecule in the deacylation process. Site-directed mutagenesis and crystallographic studies on both enzymes (*42*−*48*) have indicated that the lysine of motif 1 (respectively Lys67 and Lys65) would play mainly an electrostatic role. Finally, the newly solved structure of the Henri−Michaelis complex of R61 with a highly specific fragment of cell wall precursor probes

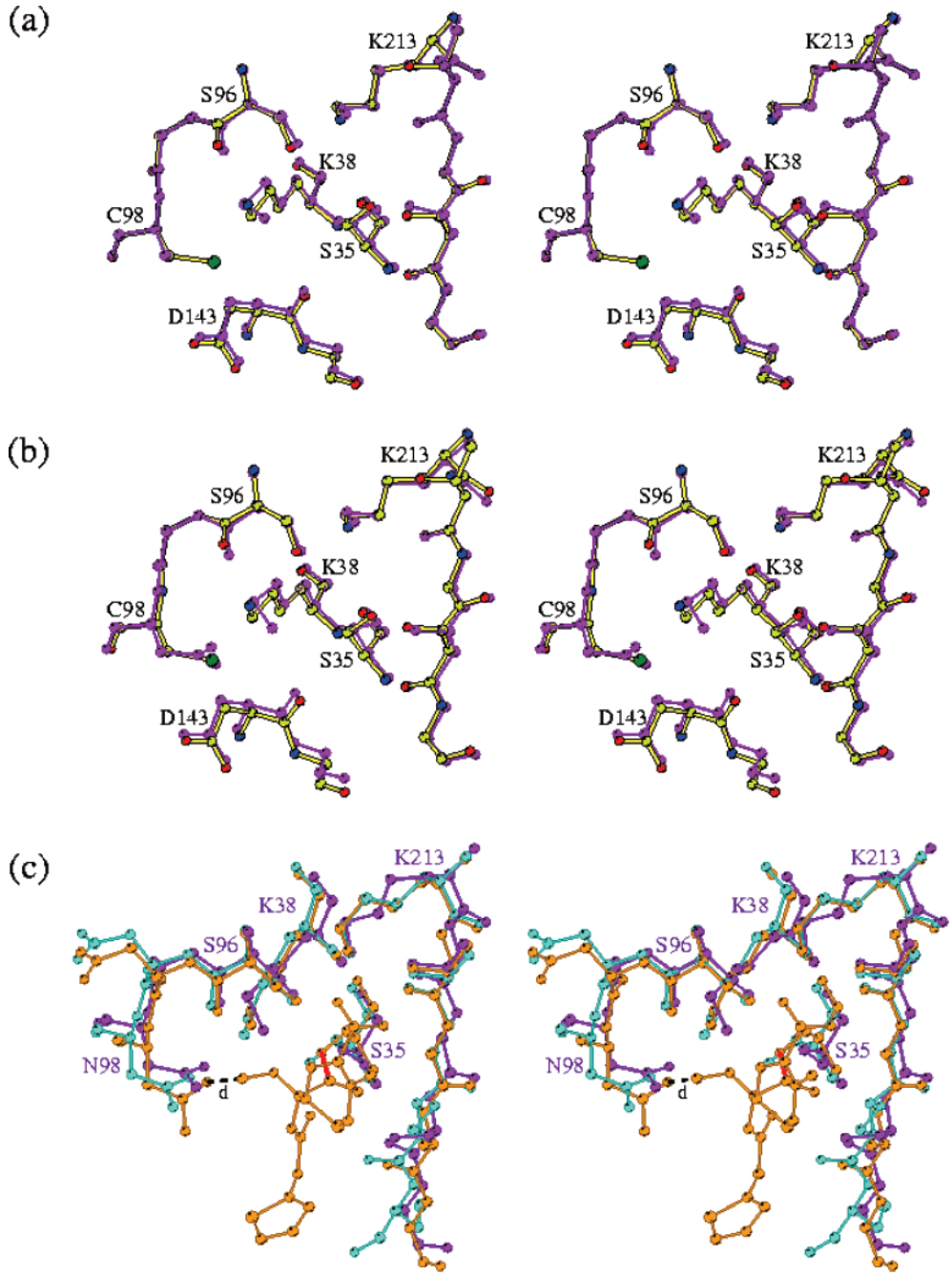

FIGURE 3: Superimposed active sites of (a) the K15 wild-type enzyme and its Cys98Ala mutant (magenta), (b) the K15 wild-type enzyme and its C98N mutant (magenta), and (c) the K15 Cys98Asn mutant (magenta), the NMCA class A β-lactamase (*38*) (cyan), and the acyl-enzyme adduct formed by the BS3 class A β-lactamase with cefoxitin (orange) (*59*). In the BS3−cefoxitin structure, the distance *d* is equal to 2.8 Å.

the role played by the conserved asparagine residue in motif 2 (Asn161) as a H-bond donor for a correct orientation of peptide substrates and antibiotics (*55*).

The catalytic site of the class D β-lactamases exhibits some very specific features when compared to the other penicilloyl serine transferases. First, it has a significant hydrophobic character with a conserved valine residue (Val117) replacing the conserved asparagine residue in motif 2, with the conserved dyad Trp154-Leu/Ile155 in the corresponding Ω-like loop, and with a mostly conserved hydrophobic residue (Trp/Phe/Ala) in position 208, downstream of the Lys-Thr-Gly triad motif 3. Depending on pH values, the lysine residue of motif 1 (Lys70) undergoes a carbonatation reaction. It has been demonstrated that the activity of class D β-lactamases is strongly related to the modification of this lysine. X-ray structures of class D enzymes solved at different pH values have shown that the carbonated lysine of motif 1 clearly plays an important structural role by conferring a functional geometry to the active site. It has also been proposed to be the general base that activates the nucleophilic serine hydroxyl group for acylation and the incoming hydrolytic water for the deacylation step, following a symmetrical mechanism for hydrolysis (*49*).

The active sites of the penicillin-binding module of class B PBPs [*Enterococcus faecium* PBP5r (*51*), *Streptococcus pneumoniae* PBP2x (*52*), and *Staphylococcus aureus* PBP2a* (*53*)] and of monofunctional PBPs of the Ser-Xaa-Asn type [*E. coli* PBP5 (*50*) and *Streptomyces* K15 DD-transpeptidase

(*14*)] present another situation since there are no residues equivalent to Glu166 of class A β-lactamases nor to Tyr150 of class C β-lactamases or to the carbonated Lys70 of class D β-lactamases. In agreement with the distances between the conserved residues observed in the active sites of the different available PBP X-ray structures, one may assume a common mechanism for acylation.

Replacement of Lys38 by His in motif 1 or conversion of Ser96 into Ala in motif 2 had no important effect on the active site geometry of the K15 DD-transpeptidase/PBP. However, marked differences were observed with respect to their catalytic activities. Both mutations almost completely abolish the penicillin-binding activity and severely impair the transpeptidation activities. The hydrolysis of thiolester substrates by the Ser96Ala mutant is less altered than with the Lys38/His mutant. These results indicate that Lys38 and Ser96 are essential elements of the catalysis. They are also in general agreement with those obtained for other PBPs. The effects of mutation of Lys in motif 1 or Ser in motif 2 of *E. coli* PBP2 (*54*) are very similar to those observed with the K15 enzyme. The substitution of Lys47 by Arg in motif 1 of *E. coli* PBP5 gives rise to a protein that has no carboxypeptidase activity and poor penicillin-binding activity (0.2% compared to the wild-type enzyme) (*55*). The replacement of Ser110 by Ala, Thr, or Glu in motif 2 of *E. coli* PBP5 abolishes the carboxypeptidase activity and reduces the penicillin-binding activity to 1% or less when compared to that of the wild-type enzyme (*55*).

The structures of the wild-type K15 enzyme and of the four mutants described here show that the active serine Ser35 has an unusual conformation where the hydroxyl group is 5 Å away from Lys38. The same observation is also made in the structure of the Lys73His mutant of the *S. aureus* class A β-lactamase (*56*) and monomer B of the methicillin-resistant *S. aureus* PBP2a*, where the active serine side chains (respectively Ser70 and Ser403) adopt an alternative conformation orienting the hydroxyl group toward the carbonyl of the serine of motif 3 (respectively Ser235 and Ser598). As in the K15 enzyme, it thus points toward the oxyanion hole (Figure 2b). In the case of the Lys73His *S. aureus* β-lactamase, it was concluded that the histidine ring was positioned so that it was unable to interact with the catalytic serine in contrast to the situation in the wild-type structure where Lys73 is hydrogen-bonded to Ser70. Thus the hydroxyl group of Ser70 was not correctly positioned for an efficient nucleophilic attack on the substrate, resulting in a drastic drop in activity. In the *S. aureus* PBP2a*, the poor acylation rate [k_2/K of 12 $M^{-1}\cdot s^{-1}$ for benzylpenicillin (*57*)] is due to a distorted active site which must undergo a conformational adaptation for acylation to occur. The acyl-PBP2a* structures show that binding of the β-lactam compounds requires a 1.8 Å move of the active site serine Oγ and a twisting of the β3 strand with an enlargement of the catalytic pocket. The K15 enzyme represents to some extent an intermediate case. Indeed, its catalytic machinery is not very efficient when compared to other PBPs, yet it does catalyze transpeptidation reactions as well as acylation by β-lactams. With a k_2/K of 135 $M^{-1}\cdot s^{-1}$ rate constant for enzyme acylation by benzylpenicillin, K15 may be considered as a PBP of intermediate penicillin sensitivity. We observe that the overall topology of its active site is more similar to that of a class A β-lactamase or of the acylated forms of *E. faecium* PBP5r and *S. aureus* PBP2a*. But, on the other hand, the hydrogen-bonding network in the active site of K15 is completely similar to that found in monomer B of the apo *S. aureus* PBP2a*.

In the wild-type K15 enzyme, Lys38 is at H-bond distance from Ser96 and Cys98 of motif 2. The structure of the Lys38His mutant shows that the histidine side chain cannot replace that of lysine in its interactions with the residues of motif 2. Binding studies of radiolabeled benzylpenicillin performed with the Lys38His mutant at different pH values (from 3.0 to 12.0) have shown that the penicillin-binding activity is always lost. It thus appears that an unprotonated His38 cannot successfully play the role of general base attributed to the ϵ-amino group of the lysine. The almost complete loss of activity of the Lys38His mutant may be explained by the double penalty of the position of the Ser35 side chain unsuitable for an efficient nucleophilic attack and the impossibility for the His38 side chain to act as the base for abstraction/back-donation of a proton during the acylation mechanism.

In the wild-type enzyme, Ser96 is hydrogen-bonded to both Lys38 and Lys213, allowing a good orientation of its hydroxyl group to possibly participate in the protonation of the leaving group. In the Ser96Ala mutant structure, the hydroxyl group of Ser96 is replaced by a water molecule (Wat524) that is hydrogen-bonded to Lys38 and Lys213. It could then replace to some extent the Ser96 side chain in the catalytic mechanism.

On the basis of these data, a potential acylation pathway can be proposed (Scheme 3). Activation of the nucleophilic Ser35 residue by Lys38 could be assisted by the α2 helix dipole and the polarized carbonyl group of the substrate ($R_1-CONH-R_2$) hydrogen-bonded to the oxyanion hole. Ser96 would be a key intermediate in the proton transfer from the Ser35 hydroxyl to the nitrogen atom of the substrate leaving group via Lys38 during acylation. The high-resolution structure of the nitrocefin−acyl-PBP2a* of the *S. aureus* complex (*53*) shows that the hydroxyl group of the conserved serine of motif 2 (Ser462) is hydrogen-bonded to the amino group of the lysine side chain of motif 1 (Lys406). Most likely, in this case, lysine of motif 1 abstracts a proton from the active site serine. The abstracted proton could then be back-donated by the lysine to the β-lactam leaving group nitrogen via the serine of motif 2.

The K15 enzyme has a unique Ser-Gly-Cys motif 2 since the most common situation is an asparagine residue in the third position, with the exception of the class D β-lactamases which have a strictly conserved valine residue. The substitution of an asparagine by a serine in PBPs results in a decreased acylation rate with the peptide substrates, the effect being less marked for the thiolester substrates and the β-lactams (*55*, *58*). The interaction of the K15 enzyme with the peptide substrates is strongly affected by the two Cys98Ala/Asn mutations. These two mutants exhibit a higher catalytic activity with the thiolester substrates. In the same way, one almost systematically observes increased acylation and deacylation rates with the β-lactams, except for cefoxitin with the Cys98Ala mutant. The Cys98Asn mutation is thus accompanied by a modification of specificity with respect to antibiotics. The example of cefoxitin is most striking. In the structure of the Cys98Asn mutant, the asparagine residue has a relative position more or less equivalent to that of

Scheme 3: Possible Acylation Pathway

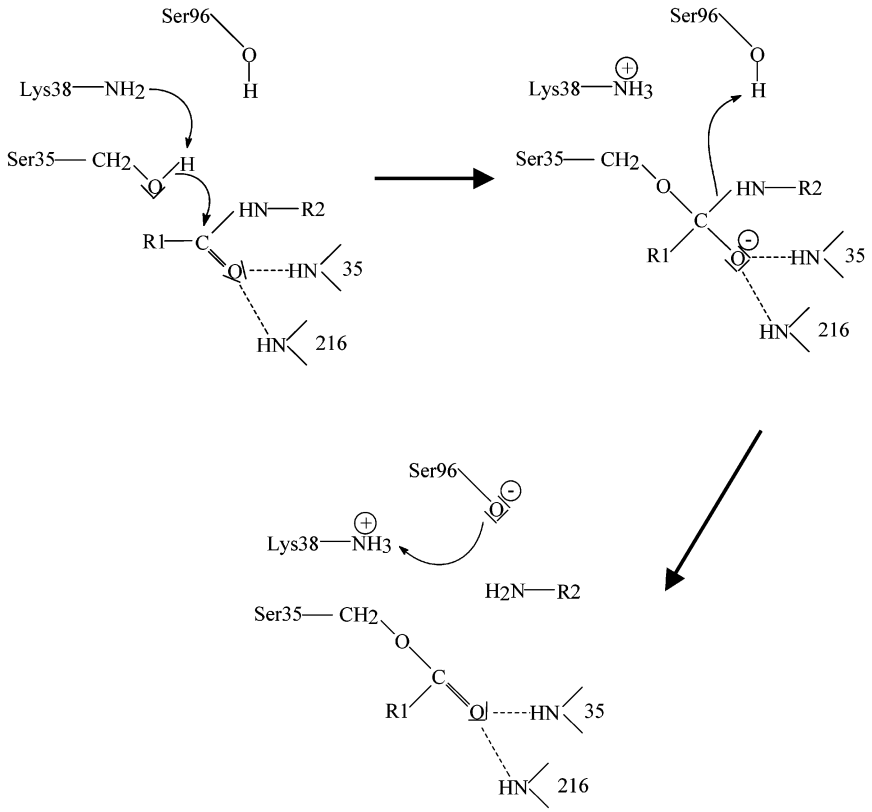

Asn132 in the NMCA class A carbapenemase from *E. cloacae* (*38*). It would make more favorable interactions with the 7α-methoxy group, allowing a better stabilization of cefoxitin in the active site as illustrated by Figure 3c. One can conclude that a cysteine residue in position 98 is overall less favorable than an asparagine for an adequate positioning of the thiolester substrates and the *β*-lactam and that the presence of an asparagine to some extent allows restoration to an environment similar to that of other penicilloyl serine transferases. On the opposite hand and as observed for other PBPs, the transpeptidation reaction, which is the physiological function, is much more sensitive to both mutations. Surprisingly, the presence of an asparagine side chain significantly reduces the catalytic efficiency with the peptide substrate.

Since there is no counterpart in the K15 enzyme to the class A Glu166, the class C Tyr150, or the class D carbonated Lys70, which are likely the key residues in a symmetrical hydrolysis mechanisms, which residue can be the candidate for activating the catalytic water molecule that would attack the penicilloyl-enzyme carbonyl? In the *Streptomyces* R61 PBP, it has been suggested that Tyr159 is in a favorable orientation for the recruitment of a deacylating water molecule, as seen in the class C *β*-lactamases (*48*). On the basis of the data obtained for the Lys38His and Ser96Ala K15 mutants, it is possible that both Lys38 and Ser96 can be involved in the transfer of the water molecule to the carbonyl of the acyl-enzyme during the deacylation step. In *E. coli* PBP5, although it appears obvious that a good positioning of the N-terminal end of the α2 helix bearing the active serine Ser44 and Lys47 is critical for the catalysis, an alternative mechanism for hydrolysis of the acyl-enzyme complex was proposed (*50*). Indeed, one may note that one structural feature is observed in all PBP structures. There is roughly a spatial equivalence of the side chain carboxyl group of Glu166 in class A *β*-lactamases with the main chain carbonyl group of one residue in the Ω-like loop: His151 in PBP5 from *E. coli*, Tyr538 in PBP5r from *E. faecium*, Phe450 in PBP2x from *S. pneumoniae*, and Tyr519 in PBP2a* from *S. aureus*. In the absence of another more powerful candidate, the backbone carbonyl moiety of those residues may participate in deacylation by more or less correctly orienting a hydrolytic water molecule.

In conclusion, site-directed mutagenesis and kinetic and crystallographic studies of the *Streptomyces* K15 DD-transpeptidase bring significant information to the understanding of the catalytic mechanism of PBPs and consolidate the observation that obviously the conservation of the catalytic cleft residues in the penicilloyl serine transferases does not imply the conservation of their roles in the reaction mechanism or even the conservation of the reaction mechanism itself.

ACKNOWLEDGMENT

We thank Prof. A. Lewitt-Bentley for expert assistance during data collection at beamline D41A at LURE (France). We also thank the staff of beamline ID14-3 at ESRF (France).

REFERENCES

1. van Heijenoort, J. (2001) *Glycobiology 11*, 25R−36R.
2. Terrak, M., Ghosh, T. K., van Heijenoort, J., Van Beeumen, J., Lampilas, M., Aszodi, J., Ayala, J. A., Ghuysen, J.-M., and Nguyen-Distèche, M. (1999) *Mol. Microbiol. 34*, 350−364.
3. Vollmer, W., von Rechenberg, M., and Höltje, J. V. (1999) *J. Biol. Chem. 274*, 6726−6734.

4. Marrec-Fairley, M., Piette, A., Gallet, X., Brasseur, R., Hara, H., Fraipont, C., Ghuysen, J.-M., and Nguyen-Distèche, M. (2000) *Mol. Microbiol. 37*, 1019−1031.
5. Adam, M., Fraipont, C., Rhazi, N., Nguyen-Distèche, M., Lakaye, B., Frère, J.-M., Devreese, B., Van Beeumen, J., van Heijenoort, J., and Ghuysen, J.-M. (1997) *J. Bacteriol. 179*, 6005−6009.
6. Goffin, C., and Ghuysen, J.-M. (1998) *Microbiol. Mol. Biol. Rev. 62*, 1079−1093.
7. Höltje, J. V. (1998) *Microbiol. Mol. Biol. Rev. 62*, 181−203.
8. Nelson, D. E., and Young, K. D. (2001) *J. Bacteriol. 183*, 3055−3064.
9. Frère, J.-M. (1995) *Mol. Microbiol. 16*, 385−395.
10. Ghuysen, J.-M., and Dive, G. (1994) *New Compr. Biochem. 27*, 103−130.
11. Palomeque-Messia, P., Quittre, V., Leyh-Bouille, M., Nguyen-Distèche, M., Gershater, C. J. L., Dacey, I. K., Dusart, J., Van Beeumen, J., and Ghuysen, J.-M. (1992) *Biochem. J. 288*, 87−91.
12. Nguyen-Distèche, M., Leyh-Bouille, M., Pirlot, S., Frère, J.-M., and Ghuysen, J.-M. (1986) *Biochem. J. 235*, 167−176.
13. Grandchamps, J., Nguyen-Distèche, M., Damblon, C., Frère, J.-M., and Ghuysen, J.-M. (1995) *Biochem. J. 307*, 335−339.
14. Fonzé, E., Vermeire, M., Nguyen-Distèche, M., Brasseur, R., and Charlier, P. (1999) *J. Biol. Chem. 274*, 21853−21860.
15. Matagne, A., and Frère, J.-M. (1995) *Biochim. Biophys. Acta 1246*, 109−127.
16. Minasov, G., Wang, X., and Shoichet, B. K. (2002) *J. Am. Chem. Soc. 124*, 5333−5340.
17. Kelly, J. A., Knox, J. R., Zhao, H., Frère, J.-M., and Ghuysen, J.-M. (1989) *J. Mol. Biol. 209*, 281−295.
18. Jamin, M., Wilkin, J. M., and Frère, J.-M. (1995) *Essays Biochem. 29*, 1−24.
19. Knox, J. R., Moews, P. C., and Frère, J.-M. (1996) *Chem. Biol. 3*, 937−947.
20. Paetzel, M., Danel, F., De Castro, L., Mosimann, S. C., Page, M. G. P., and Strynadka, N. C. J. (2000) *Nat. Struct. Biol. 7*, 918−925.
21. Maveyraud, L., Golemi, D., Kotra, L. P., Tranier, S., Vakulenko, S., Mobashery, S., and Samama, J. P. (2000) *Struct. Folding Des. 8*, 1289−1298.
22. Delettre, J., Jarlier, V., Collatz, E., and Sougakoff, W. (2001) *J. Mol. Biol. 310*, 859−884.
23. Adam, M., Damblon, C., Plaitin, B., Christiaens, L., and Frère, J.-M. (1990) *Biochem J. 270*, 525−529.
24. Adam, M., Damblon, C., Jamin, M., Zorzi, W., Dusart, V., Galleni, M., El Kharroubi, A., Piras, G., Spratt, B. G., Keck, W., Coyette, J., Ghuysen, J.-M., Nguyen-Distèche, M., and Frère, J.-M. (1991) *Biochem. J. 279*, 601−604.
25. Katz, E., Thompson, C. J., and Hopwood, D. A. (1983) *J. Gen. Microbiol. 129*, 2703−2714.
26. Ho, S. N., Hunt, H. D., Horton, R. M., Pullen, J. K., and Pease, L. R. (1989) *Gene 77*, 51−59.
27. Hopwood, D. A., Kieser, T., Wright, H. M., and Bibb, M. J. (1993) *J. Gen. Microbiol. 129*, 2257−2269.
28. Granier, B., Jamin, M., Adam, M., Galleni, M., Lakaye, B., Zorzi, W., Grandchamps, J., Wilkin, J.-M., Fraipont, C., Joris, B., Duez, C., Nguyen-Distèche, M., Coyette, J., Leyh-Bouille, M., Dusart, J., Christiaens, L., Frère, J.-M., and Ghuysen, J.-M. (1994) *Methods Enzymol. 244*, 249−266.
29. Jamin, M., Adam, M., Damblon, C., Christiaens, L., and Frère, J.-M. (1991) *Biochem. J. 280*, 499−506.
30. Leyh-Bouille, M., Nguyen-Distèche, M., Pirlot, S., Veithen, A., Bourguignon, C., and Ghuysen, J.-M. (1986) *Biochem. J. 235*, 177−182.
31. Fraipont, C., Adam, M., Nguyen-Distèche, M., Keck, W., Van Beeumen, J., Ayala, J. A., Granier, B., Hara, H., and Ghuysen, J.-M. (1994) *Biochem. J. 298*, 189−195.
32. Siemens Industrial Automation, Inc. (1993) *SAINT Software Reference Manual*, Madison, WI.
33. Leslie, A. G. R. W. (1996) *MOSFLM Version 5.40 Mosflm Users Guide*.
34. Collaborative Computing Project (1994) *Acta Crystallogr. D50*, 760−763.
35. Kabsch, W. (1993) *J. Appl. Crystallogr. 26*, 795−800.
36. Brünger, A. T. (1993) *X-PLOR Version 3.1: A System for X-ray Crystallography and NMR*, Yale University Press, New Haven, CT.
37. Roussel, A., and Cambillau, C. (1989) *Silicon Graphics Geometry Partner Directory*, pp 77−78, Silicon Graphics, Mountain View, CA.
38. Mourey, L., Kotra, L. P., Bellettini, J., Bulychev, A., O'Brien, M., Miller, M. J., Mobasherry, S., and Samama, J.-P. (1999) *J. Biol. Chem. 274*, 25260−25265.
39. Jacob, F., Joris, B., Lepage, S., Dusart, J., and Frere, J.-M. (1990) *Biochem. J. 271*, 399−406.
40. Jacob, F., Joris, B., Dideberg, O., Dusart, J., Ghuysen, J.-M., and Frere, J.-M. (1990) *Protein Eng. 4*, 79−86.
41. Juteau, J.-M., Billings, E., Knox, J. R., and Levesque, R. C. (1992) *Protein Eng. 5*, 693−701.
42. Josuna, J., Viadiu, H., Fink, A., and Soberón, X. (1995) *J. Biol. Chem. 270*, 775−780.
43. Tsukumoto, K., Tachibana, K., Yamazaki, N., Ishii, Y., Ujiie, K., Nishida, N., and Sawai, T. (1990) *Eur. J. Biochem. 188*, 15−22.
44. Monnaie, D., Dubus, A., Cooke, D., Marchand-Brynaert, J., Normark, S., and Frere, J.-M. (1994) *Biochemistry 33*, 5193−5201.
45. Beadle, B. M., and Shoichet, B. K. (2002) *J. Mol. Biol. 321*, 285−296.
46. Hadonou, A. M., Jamin, M., Adam, M., Joris, B., Dusart, J., Ghuysen, J.-M., and Frere, J.-M. (1992) *Biochem. J. 282*, 495−500.
47. Crichlow, C. V., Kuzin, A. P., Nukaga, M., Sawai, T., and Knox, J. R. (1999) *Biochemistry 38*, 10256−10261.
48. McDonough, M. A., Anderson, J. W., Silvaggi, N. R., Pratt, R. F., Knox, J. R., and Kelly, J. A. (2002) *J. Mol. Biol. 322*, 111−122.
49. Golemi, D., Maveyraud, L., Vakulenko, S., Samama, J.-P., and Mobasherry, S. (2001) *Proc. Natl. Acad. Sci. U.S.A. 98*, 14280−14285.
50. Davies, C., White, S. W., and Nicholas, R. A. (2001) *J. Biol. Chem. 276*, 616−623.
51. Gordon, E., Mouz, E., Duée, E., and Dideberg, O. (2000) *J. Mol. Biol. 299*, 477−485.
52. Sauvage, E., Schoot, B., Marquette, J. P., Leonard, G., Stefanic, P., Kerff, F., Fonzé, E., Taburet, Y., Prevost, D., Dumas, J., Coyette, J., and Charlier, P. (2002) *Cell. Mol. Life Sci. 59*, 1223−1232.
53. Lim, D., and Strynadka, N. (2002) *Nat. Struct. Biol. 9*, 870−876.
54. Adahi, H., Ishiguro, M., Imajoh, S., Ohta, T., and Matsuzawa, H. (1992) *Biochemistry 31*, 430−437.
55. Van der Linden, M. P. G., de Haan, L., Dideberg, O., and Keck, W. (1994) *Biochem. J. 303*, 357−362.
56. Chen, C. C., Smith, T. J., Kapadia, G., Wäsch, S., Zawadzeke, L. E., Coulson, A., and Herzberg, O. (1996) *Biochemistry 35*, 12251−12258.
57. Graves-Woodward K., and Pratt, R. F. (1998) *Biochem. J. 332*, 755−761.
58. Wilkin, J. M., Jamin, M., Joris, B., and Frere, J.-M. (1993) *Biochem. J. 293*, 195−201.
59. Fonzé, E., Vanhove, M., Dive, G., Sauvage, E., Frère, J.-M., and Charlier, P. (2002) *Biochemistry 41*, 1877−1885.

BI027256X